Spectrochimica Acta, Vol. 31A, pp. 1329 to 1341. Pergamon Press, 1975. Printed in Northern Ireland

Vibrational analysis of 1-halo-1,3-pentadiynes $CH_3—C{\equiv}C—C{\equiv}C—X$ (X = Cl, Br and I). Coriolis coefficients of 1-chloro, 1-bromo- and of unsubstituted 1,3-pentadiyne

LEIF BENESTAD, ELSE AUGDAHL and ELSE KLOSTER-JENSEN
Department of Chemistry, University of Oslo, Oslo 3, Norway

(*Received* 21 *October* 1974)

Abstract—The i.r. and Raman spectra of the series $CH_3—C{\equiv}C—C{\equiv}C—X$ (X = Cl, Br and I) were examined in solution (4000–50 cm^{-1}) and as solids at low temperature. Infrared vapour spectra were recorded (4000–350 cm^{-1}) and Coriolis coefficients were determined for $CH_3—C{\equiv}C—C{\equiv}C—X$ (X = H, Cl and Br). The syntheses of the compounds are reported.

INTRODUCTION

This paper presents the vibrational analyses of the three 1-halo-1,3-pentadiynes

$$CH_3—C{\equiv}C—C{\equiv}C—X$$

(X = Cl, Br and I). The molecules will hereafter be called (Cl), (Br) and (I), respectively. Vibrational assignments were further made for the parent compound $CH_3—C{\equiv}C—C{\equiv}C—H$(H). After completion of the present work, however, results for the latter molecule have been published [1]. Good agreement was found to exist between these two independent studies. We also examined the resolved rotational structure of the perpendicular CH_3 bands and calculated Coriolis constant ζ_i for (H), (Cl) and (Br). In a recent paper we have published force constants, mean amplitudes and ζ_i values as derived from the force field [2]. Furthermore, the syntheses of the $CH_3—C{\equiv}C—C{\equiv}C—X$ series is reported in detail.

Vibrational analyses of the 1-halopropynes

$$CH_3—C{\equiv}C—X$$

(X = Cl, Br, I) [3, 4] as well as previous work on monohalodiacetylenes

$$H—C{\equiv}C—C{\equiv}C—X$$

(X = Cl, Br, I) [5, 6] were useful in making the assignments.

EXPERIMENTAL

Chemicals

A general procedure was followed as described [7]. The reactions were performed in an atmosphere of nitrogen. MS-pure samples of the products in minor quantities have been obtained in earlier preparations [8]. All m.p.'s are uncorrected.

1,3-*Pentadiyne* [9] was prepared as follows: Freshly prepared and resublimed butadiyne [10] (6·02 g, 0·12 mole) was dissolved in dry ether (25 ml) and added dropwise to lithium amide (from 0·85 g met. Li) in liquid ammonia (150 ml) under stirring at −40°. After stirring for another 10 min methyl iodide (20 g, 0·14 mole) in ether (15 ml) was added in a dropwise manner and strirring was continued for 10 min. Most of the ammonia was allowed to evaporate through a cellophane membrane overnight, ether (150 ml) was added, followed by a saturated aqueous solution of ammonium chloride under stirring at −50°. The ether phase was removed, and extraction under stirring with ether (50 ml) was repeated four times. The combined ether extracts, dried over sodium sulfate were subjected to fractional distillation at −45°/10 torr. The product concentrated in the last fraction (−45°—room temp.; 15 ml) which after gas liquid chromatography at 65° yielded 2·39 g (31 %) 1,3-pentadiyne of purity *ca.* 97 %. A second GLC yielded a highly pure product, m.p. −31·5–30·5°, vapour pressure 27·5 torr/0°.

Residual solids were sublimed into a vacuum tube, dissolved in ether and gas chromatographed once, yielding 350 mg of MS pure 2,4-hexadiyne [10–12].

1-*Chloro*-1,3-*pentadiyne*. 1,3-pentadiyne (500 mg, 7·8 m-mole, 1*x* GLC) in dry ether (10 ml) was added dropwise to butyl lithium (7·8 m mole) in ether (50 ml) at −30°. A *ca.* 15 % solution of molecular chlorine in Freon-11 (distilled over P_2O_5) was added at −40° until the reaction was no longer basic. Fractional distillation of the reaction mixture at −45°/10 torr and GLC of the last fraction (8 ml) at 65° (retention time 28 min) gave 455 mg (59·4 %) of 1-chloro-1,3-pentadiyne. A second GLC yielded 400 mg and a third GLC at 50°

(retention time 51 min) furnished 350 mg of highly pure product, m.p. −9 to −8°.

1-*Bromo*-1,3-*pentadiyne* [13–15]. 1,3-Pentadiyne (300 mg 4·7 m-mole) in 10 ml of dry ether was added to phenyl lithium (4·7 m-mole) in dry ether (50 ml) at −50°. A weighed amount of bromine (0·76 g, 4·7 m-mole) was added until neutral reaction (almost quantitatively). Working up as for 1-chloro-1,3-pentadiyne and GLC at 105° (retention time 25 min) yielded 240 mg (35·7 %) of 1-bromo-1,3-pentadiyne, which after a second GLC gave 145 mg of product, m.p. 16·5–17·0° (5·1° [13]).

1-*iodo*-1,3-*pentadiyne* [9]. Iodine (2·08 g, 8·2 m-mole) was introduced in portions into liquid ammonia (*ca.* 40 ml) at −50°. 1,3-Pentadiyne (525 mg, 8·2 m-mole) in dry ether (10 ml) was added under stirring during 15 min. Stirring was continued for another 30 min, at which time the reaction mixture turned water clear. Most of the ammonia was evaporated through a cellophane membrane, ether (50 ml) was added, followed by water (50 ml) under vigorous stirring. The ether phase was removed and the aqueous layer was extracted by thorough stirring with ether (4 × 30 ml). The dried, combined ether extracts were fractionated as above, and the solid colourless residue was sublimed at $20°/10^{-2}$ torr into a vacuum tube cooled in liquid nitrogen. Fraction 1 (1·57 g) contained some ether and was refractionated leaving 0·90 g colourless residue. Fraction 2 (0·64 g) was resublimed over phosphorus pentoxide into vacuum tubes cooled at −80°. After a first fraction of 0·22 g, the second fraction of 0·42 g 1-iodo-1,3-pentadiyne showed m.p. 34·8–35·2° (34–35° [9]), yield *ca.* 95 %.

Preparation of this compound according to [9] from 1·4-di-chloro-2-butyne, 3 equivalents of sodium amide, and further methyliodide and iodine, furnished a product slightly contaminated with 2,4-hexadiyne. Attempts on GLC of 1-iodo-1,3-pentadiyne were unsuccessful.

Instrumental

The i.r. spectra were recorded with a Perkin–Elmer model 225 spectrometer calibrated against standard lines of various gases [16, 17]. Far i.r. spectra were obtained with a Perkin–Elmer/Hitachi FIS spectrometer. A Cary 81 Raman spectrometer equipped with a Spectra Physics model 125 He–Ne laser was employed for recordings of solutions (standard capillary tubes and the 180° illumination mode). The Raman solid spectra were obtained using a CRL 52 G argon-ion laser, 5145 Å and 90° illumination.

A 10 cm cell with CsI windows and a 1 m cell equipped with KRS-5 windows were used in the recordings of the vapour spectra. Infrared spectra were also obtained from *ca.* 20 % solutions in CCl_4 and CS_2 using KBr cells of thickness 0·1 mm. In the far i.r. *ca.* 10 % pentane solutions were studied in 0·5 mm polyethylene cells. Vapour spectra were not available in this region. *Ca.* 40 % solutions in CCl_4 or C_6H_6 were employed for the Raman recordings. All solutions were prepared by distilling the sample into the precooled solvent on a vacuum line. Discolouration of all the solutions took place at ambient temperature, and spurious bands were observed in the i.r. spectra of (Br) and (I). Therefore the compounds were also examined at low temperatures. For this purpose samples were vacuum transferred to a CsI window (i.r.) or a copper tip (Raman) [18] in a cryostat cooled with liquid nitrogen.

SYMMETRY

The symmetry point group C_{3v} was assumed for these molecules which possess fourteen normal vibrations all allowed in both the i.r. and the Raman spectra. Of these seven will belong to species a_1, giving rise to parallel bands in the i.r. and polarized bands in the Raman effect. The remaining seven fundamentals will be of species e, appearing as perpendicular bands in the i.r. and depolarized bands in the Raman spectrum.

RESULTS AND DISCUSSION

A microwave investigation of (H) had shown this molecule to be a symmetric top with a value of 0·0679 cm^{-1} for B'', the smaller of the two rotational constants [19]. The following structural parameters were employed to calculate A'' and B'' for the 1-halo derivatives: (C—H), 1·097 Å; ∠HCC, 108·23° [20]; (C—C), 1·458 Å, (C≡C), 1·207 Å [21]; (≡C—C≡), 1·375 Å; (C—Cl), 1·635 Å, (C—Br) 1·793 Å and (C—I), 1·991 Å [5]. The resulting values of B'', 0·025 cm^{-1} (Cl), 0·018 cm^{-1} (Br) and 0·015 cm^{-1} (I) together with the A'' value of 5·29 cm^{-1} were used to calculate ζ_t and A' for the perpenducular CH_3 vibrations and to estimate the band contours and P—R separations of the parallel bands [22, 23]. The Q branch of the latter should be too weak to be observed, as verified by the experiments. The following P—R separations were predicted: 7 cm^{-1} (Cl), 6 cm^{-1} (Br) and 5 cm^{-1} (I). A resolved rotational structure might be expected for the e-type CH_3 fundamentals

Table 1. Infrared and Raman spectral data for 1-chloro-1,3-pentadiyne.

Infrared			Raman			
Gas	Solution (CCl_4)	Solid	Solution†	Solid	Interpretation*	
	101 s‡				$\nu_{14}(e)$ fund	
			199 vw		$2\nu_{14} = 202$	$A_1 + E$
~238 m	241 m	249 s	242 s D	247 s	$\nu_{13}(e)$ fund	
		305 w	296 vw	305 w	$3\nu_{14} = 303$	$A_1 + A_2 + 2E$
		333 w, sh				
339 m	339 s	343 vs	340 w	342 m	$\nu_{12}(e)$ fund	
374 381 m ‖					$\nu_{11} - \nu_{14} = 356$	$A_1 + A_2 + E$
425 w	437 w	444 m	435 w, sh	443 w, sh	$\nu_7(a_1)$ fund	
	457 w	458 w	458 vs D	457 vs	$\nu_{11}(e)$ fund	
				478 w		
485 w	500 w	508 m	498 w, sh	503 w	$2\nu_{13} = 482$	$A_1 + E$
			520 vw			
543 549 m ‖	547 w, sh				$\nu_{11} + \nu_{14} = 558$	$A_1 + A_2 + E$
565 572 m ‖	579 s	588 s		589 w	$\nu_{12} + \nu_{13} = 580$	$A_1 + A_2 + E$
	655 vw	663 vw	657 vvw	662 vw	$\nu_{11} + 2\nu_{14} = 659$	$A_1 + A_2 + 2E$
690 w	682 m	692 m			$\nu_7 + \nu_{13} = 678$	E
			~690 vw	692 w	$\nu_{11} + \nu_{13} = 698$	$A_1 + A_2 + E$
748 w			734 vw			
794 801 m ‖	791 m§	795 m	795 vvw	796 vw	$\nu_{11} + \nu_{12} = 796$	$A_1 + A_2 + E$
	809 w, sh	804 w, sh				
859 865 s ‖	859 vs	858 vs		862 vw	$\nu_6(a_1)$ fund	
		884 vw			$2\nu_7 = 874$	A_1
		914 vw		910 w, sh	$2\nu_{11} = 914$	$A_1 + E$
	920 w	922 w	922 vw	926 w	$2\nu_{12} + \nu_{13} = 919$	$A_1 + A_2 + 2E$
				945 vw	$\nu_{11} + 2\nu_{13} = 939$	$A_1 + A_2 + 2E$
1029 w ⊥‖	1023 m	1022 s	1022 w	1025 m	$\nu_{10}(e)$ fund	
		1102 w, bd		1103 vw	$\nu_6 + \nu_{13} = 1100$	E
	1220 w, sh	1220 w, sh			hot band	
1224 1232 s ‖	1231 vs	1234 vs	1232 w	1238 m	$\nu_5(a_1)$ fund	
	1262 w	1268 w			$\nu_{10} + \nu_{13} = 1264$	$A_1 + A_2 + E$
	1292 vw	1301 w			$\nu_6 + \nu_7 = 1296$	A_1
	1362 m	1363 m	1363 vw, sh	1364 w, sh	$\nu_{10} + \nu_{12} = 1362$	$A_1 + A_2 + E$
1378 1384 s ‖	1378 s		1378 s P	1377 s	$\nu_4(a_1)$ fund	
1446 s ⊥‖	1433 s, bd	1431 s	1438 w	1432 m	$\nu_9(e)$ fund	
	1481 vw, sh	1478 vw			$\nu_{10} + \nu_{11} = 1480$	$A_1 + A_2 + E$
	1670 vw, bd				$\nu_5 + \nu_7 = 1668$	A_1
	1734 w, bd					
	1775 vw				$\nu_9 + \nu_{12} = 1772$	$A_1 + A_2 + E$
	1835 vvw				$\nu_4 + \nu_{11} = 1835$	E
2042 2049 w ‖	2037 m	2032 w	2038 vw		$2\nu_{10} = 2046$	$A_1 + E$
2074 2080 w ‖	2077 m	2074 m	2075 vw	2079 w	$\nu_5 + \nu_6 = 2090$	A_1
	2128 vw, sh	2117 w		2110 w		

* Combination frequencies and overtones are calc. from i.r. solution data. s, m, w = strong, medium, weak, v = very, bd = broad, sh = shoulder, var = variable, P, D = polarized, depolarized. ‖ = parallel and ⊥ = perpendicular contours.

† C_6H_6 solution below 1000 cm^{-1}, CCl_4 solution above 1000 cm^{-1}.

‡ n-pentane solution.

§ CS_2 solution.

‖ ν_0 calculated from K fine structure.

Table 1. *(continued)*

Gas	Infrared Solution (CCl_4)	Solid	Raman Solution†	Solid	Interpretation*	
~2152 w, sh	2149 m	2148 m	2145 vw	2145 w	hot band or ^{13}C	
2175 s	2170 vs	2168 s	2170 w	2170 m	$\nu_3(a_1)$ fund	
2238 2244 w ∥	~2234 w	2232 w		~2235 m, sh	$\nu_4 + \nu_6 = 2237$	A_1
	~2248 w			2244 m, sh	$\nu_5 + \nu_{10} = 2254$ hot band or ^{13}C	E
	2257 w	2255 w	2257 vs P	2257 vs	$\nu_2(a_1)$ fund	
	2334 vw			2331 w		
	2358 vw					
	2396 vw	2394 vw			$\nu_4 + \nu_{10} = 2401$	E
	2448 vw, sh					
	2460 w		2460 w	2467 s	$2\nu_5 = 2462$	A_1
2611 vw	2607 w	2611 vw		2607 vw	$\nu_4 + \nu_5 = 2609$	A_1
	2624 vvw					
2656 vw	2665 vw				$\nu_5 + \nu_9 = 2664$	E
				2702 w	$\nu_2 + \nu_7 = 2694$	A_1
2746 2753 w ∥	2732 m	2728 vw			$2\nu_4 = 2756$	A_1
2855 2862 m ∥	2845 s	2837 w	2847 vw	2841 m	$2\nu_9 = 2866$	$A_1 + E$
	~2874 vvw		2882 vw	2891 vw, sh		
2931 2938 s ∥	2918 s	2916 m	2917 m P	2914 s	$\nu_1(a_1)$ fund	
2977 s ⊥∥	2963 m	2960 w	2963 w	2962 s	$\nu_8(e)$ fund	
	3039 vw, bd					
	3094 w, sh					
3124 vw	3112 m	3113 w			$\nu_2 + \nu_6 = 3116$	A_1
	3159 vw					
3415 vw	3405 m	3405 w			$\nu_8 + \nu_{11} = 3420$	$A_1 + A_2 + E$
	3933 vw				$\nu_1 + \nu_{10} = 3941$	E

from the calculated ζ_i values [2] and from previous observations in $CH_3—C{\equiv}N$ [24] and

$$CH_3—C{\equiv}C—X$$

(X = H, Cl, Br and I) [3, 4, 25]. Tables 1–4 contain the proposed assignments and the vibrational spectra are presented in Figs. 1–4.

VIBRATIONAL ASSIGNMENT

50–700 cm^{-1}

Five fundamentals were expected in this region, one of species a_1 and four of species e. The former, ν_7 was readily assigned as the medium strong polarized Raman band at 357 cm^{-1} in (Br) and 310 cm^{-1} in (I). Force constant calculations based on the initial force field suggested the weak shoulder at 435 cm^{-1} as ν_7 in (Cl). Similar calculations carried out for (Br) and (I) added support to this assignment by giving values very close to those observed. A possible alternative for ν_7 in (Cl) would be the medium strong vapour band at 378 cm^{-1} showing parallel contour. However, this frequency may also be explained as the difference $\nu_{11} - \nu_{14}$, since the gas phase value of ν_{14} is likely to be shifted down by 10–20 cm^{-1} from the solution value at 101 cm^{-1}. The stronger band at 546 cm^{-1}, also having parallel contour, may be interpreted as the sum $\nu_{11} + \nu_{14}$. Similar features were observed in the vapour spectrum of (Br), where the weaker low lying band occurred at 387 cm^{-1}. This frequency is too high for ν_7 as compared to the observed solution value 357 cm^{-1}. An analogous interpretation of 387 cm^{-1} as $\nu_{11} - \nu_{14}$ and 546 cm^{-1} as the corresponding sum seems reasonable and supports our assignments in (Cl).

Except for ν_{12} in (Cl), the skeletal bending modes ν_{11}, ν_{12} and ν_{13} were recognized as medium or strong depolarized Raman bands throughout the series. The former fundamental was identified as a strong i.r. band at 339 cm^{-1}, whereas the Raman intensity was rather weak. The lowest bending mode ν_{14} appeared as strong i.r. solution bands near 100 cm^{-1} in all three molecules. Apparent from Table 4, all the skeletal deformations are rather insensitive to changes in the mass of the halogen, as previously observed for linear halodiacetylenes [5].

Table 2. Infrared and Raman spectral data for 1-bromo-1,3-pentadiyne

Infrared			Raman			
Gas	Solution (CCl_4)	Solid	Solution†	Solid	Interpretation*	
	92 s‡				$\nu_{14}(e)$ fund	
	223 m‡	236 m	225 s D	229 s	$\nu_{13}(e)$ fund	
332 m	333 s	337 vs	334 m D	335 w	$\nu_{12}(e)$ fund	
	356 vw‡	358 m	357 m P	357 m	$\nu_7(a_1)$ fund	
∼384 ∼391 m ‖					$\nu_{11} - \nu_{14} = 368$	$A_1 + A_2 + E$
	460 m	∼461 m	459 vs D	461 vs	$\nu_{11}(e)$ fund	
543 548 s ‖	558 s	570 s	558 vw	573 vw	$\nu_{11} + \nu_{14} = 552$ $\nu_{12} + \nu_{13} = 556$	$A_1 + A_2 + E$ $A_1 + A_2 + E$
	662 w	656 m			$2\nu_{12} = 666$	$A_1 + E$
	670 vw	673 w	669 w	675 w	$\nu_{11} + \nu_{13} = 683$	$A_1 + A_2 + E$
	695 vw§	698 vw	683 w	691 w	$\nu_7 + \nu_{12} = 689$	E
780 785 m ‖	780 s§	782 s		785 vw	$\nu_{11} + \nu_{12} = 793$	$A_1 + A_2 + E$
		798 w	801 vw			
812 818 m ‖	813 s§	813 s	814 w	814 w	$\nu_6(a_1)$ fund	
	859 vw	850 w				
		922 m	924 w	926 w	$2\nu_{11} = 920$	$A_1 + E$
1029 w ⊥‖	1021 m	1021 s	1021 w	1025 m	$\nu_{10}(e)$ fund	
	1075 var				Impurity	
1210 w	1212 s	1213 s	1210 m	1215 m	$\nu_5(a_1)$ fund	
	1261 var	1261 m			Impurity	
	1355 m			1356 w, sh	$\nu_{10} + \nu_{12} = 1354$	$A_1 + A_2 + E$
∼1381 m	1377 s	1371 m	1375 s P	1376 s	$\nu_4(a_1)$ fund	
1446 s ⊥‖	1433 s, bd	1427 s	1432 w	1429 m	$\nu_9(e)$ fund	
	1480 vw, sh	1482 w			$\nu_{10} + \nu_{11} = 1481$	$A_1 + A_2 + E$
	1600 vw				$\nu_4 + \nu_{13} = 1600$	E
	1713 vw				$\nu_4 + \nu_{12} = 1710$	E
	1730 w				$\nu_4 + \nu_7 = 1733$	A_1
	1755 vw				$\nu_9 + \nu_{12} = 1766$	$A_1 + A_2 + E$
			1984 vw§	1993 vw		
			2019 vw§		$\nu_5 + \nu_6 = 2025$	A_1
2040 2047 m ‖	2035 m	2031 m		2024 vw	$2\nu_{10} = 2042$	$A_1 + E$
				2068 vw		
	2114 vw, sh	2114 vw		2118 vw, sh	hot bands or ^{13}C	
		2126 w				
	2134 m	2135 s	∼2133 vw, sh			
∼2155 2161 s ‖	2146 vs	2145 vs	2144 w	2152 s	$\nu_3(a_1)$ fund	
	2158 w, sh	2154 w, sh	2154 vw, sh			
	2188 vw	2184 vw	2188 vw§	2187 w	$\nu_4 + \nu_6 = 2190$	A_1
				2222 m, sh	$\nu_5 + \nu_{10} = 2233$	E
	2232 w, sh			2232 m, sh	hot bands or ^{13}C	
	2237 w, sh	2238 vw	2239 m, sh			
∼2256 w	2244 m	2246 s	2244 vs P	2248 vs	$\nu_2(a_1)$ fund	
		2393 vw		2380 w	$\nu_4 + \nu_{10} = 2398$	E
	2421 w	2424 w	2415 w	2428 s	$2\nu_5 = 2424$	A_1
	2455 vw				$\nu_9 + \nu_{10} = 2454$	$A_1 + A_2 + E$
	2503 vw	2504 vw		2509 w	$\nu_3 + \nu_7 = 2502$	A_1
	2585 w	2584 vw		2584 vw	$\nu_2 + \nu_7 = 2600$	A_1
	2600 vw, sh			2608 w	$\nu_3 + \nu_{11} = 2606$	E
	2732 w	2730 vw	2729 vw§	2728 w	$2\nu_4 = 2754$	A_1
	2790 vw, sh	2790 vw, sh				
∼2866 w	2843 s	2833 m	2840 w	2836 m	$2\nu_9 = 2866$	$A_1 + E$
2930 2936 s ‖	2916 s	2913 m	2913 s P	2911 vs	$\nu_1(a_1)$ fund	
2975 s ⊥‖	2964 s	2959 m		2962 m	$\nu_8(e)$ fund	
	3051 m	3051 m		3053 vw	$\nu_2 + \nu_6 = 3057$	A_1
	3348 vw, sh				$\nu_3 + \nu_5 = 3358$	A_1
	3362 w	3357 w			$\nu_1 + \nu_{11} = 3376$	$A_1 + A_2 + E$
	3610 vw, bd				$\nu_2 + \nu_4 = 3621$	A_1
	3695 vw					

Footnotes: see Table 1.

Table 3. Infrared and Raman spectral data for 1-iodo-1,3-pentadiyne.

	Infrared		Raman			
Gas	Solution (CCl_4)	Solid	Solution†	Solid	Interpretation*	
	~90 s‡			93 w	$\nu_{14}(e)$ fund	
				116 w	$\nu_{12} - \nu_{13} = 119$	$A_1 + A_2 + E$
	212 w‡	225 m	214 s D	223 vs	$\nu_{13}(e)$ fund	
	302 w‡				$\nu_{13} + \nu_{14} = 304$	$A_1 + A_2 + E$
		305 s	310 m P	305 s	$\nu_7(a_1)$ fund	
$\left.\begin{matrix}328\\332\end{matrix}\right\}$ ‖ ?	333 s	334 vs	333 m	333 m	$\nu_{12}(e)$ fund	
		398 vw			$\nu_7 + \nu_{14} = 400$	E
	~433 vw		434 vw		$2\nu_{13} = 428$	$A_1 + E$
	465 m	464 m	465 s D	464 vs	$\nu_{11}(e)$ fund	
$\left.\begin{matrix}543\\548\end{matrix}\right\}$ ‖	545 s	554 m	540 vw	558 w	$\left\{\begin{matrix}\nu_{12} + \nu_{13} = 547\\ \nu_{11} + \nu_{14} = 555\end{matrix}\right.$	$A_1 + A_2 + E$ $A_1 + A_2 + E$
	~628 vw	613 vw		613 vw	$2\nu_7 = 620$	A_1
				640 vw	$\nu_7 + \nu_{12} = 643$	E
	662 vw	662 vw			$2\nu_{12} = 666$	$A_1 + E$
		670 vw	671 vw	669 w	$\nu_{11} + \nu_{13} = 679$	$A_1 + A_2 + E$
	680 vw§	676 vw		684 w	$\nu_{10} - \nu_{12} = 688$	$A_1 + A_2 + E$
	700 vw§				$2\nu_7 + \nu_{14} = 710$	E
	767 w§	765 w		769 w	$\nu_7 + \nu_{11} = 775$	E
	793 w, sh§				$\nu_{11} + \nu_{12} = 798$	$A_1 + A_2 + E$
$\left.\begin{matrix}813\\818\end{matrix}\right\}$ ‖	809 m§	808 w	811 w	808 w	$\nu_6(a_1)$ fund	
		821 vw, sh				
	~865 vw	863 vw			$\nu_7 + \nu_{11} + \nu_{14} = 865$	$A_1 + A_2 + E$
			899 vw		$\nu_6 + \nu_{14} = 899$	E
	935 vw	934 w	935 vw	936 w	$2\nu_{11} = 930$	$A_1 + E$
	1021 m	1019 s	1022 m	1024 s	$\nu_{10}(e)$ fund	
	~1068 var	1069 vw		1071 vw	impurity	
		1099 vw		1111 vw	$\nu_{10} + \nu_{14} = 1111$	$A_1 + A_2 + E$
	1198 m	1199 m	1198 m	1200 s	$\nu_5(a_1)$ fund	
	1230 vw	1239 vw			$\nu_{10} + \nu_{13} = 1235$	$A_1 + A_2 + E$
	1260 var	1261 w			impurity	
	1352 m	1352 m	1353 vw, sh	1355 w, sh	$\nu_{10} + \nu_{12} = 1354$	$A_1 + A_2 + E$
~1380	1374 s	1373 m	1375 s P	1374 s	$\nu_4(a_1)$ fund	
~1445 ⊥‖	1432 s, bd	1426 vs	1430 w	1427 m	$\nu_9(e)$ fund	
	1484 w	1480 w			$\nu_{10} + \nu_{11} = 1486$	$A_1 + A_2 + E$
				1586 vw	$\nu_4 + \nu_{13} = 1588$	E
		1652 vw		1663 vw	$\nu_5 + \nu_{11} = 1663$	E
	1766 vw	1760 vw			$\nu_9 + \nu_{12} = 1765$	$A_1 + A_2 + E$
	1900 vw				$\nu_9 + \nu_{11} = 1897$	$A_1 + A_2 + E$
	1958 w	1952 w	1957 w	1957 w	$\nu_9 + \nu_7 + \nu_{13} = 1956$	$A_1 + A_2 + E$
				2002 vw	$\nu_5 + \nu_6 = 2007$	A_1
	2032 m	2028 m		2032 vw	$2\nu_{10} = 2042$	$A_1 + E$
	2085 vw, sh	2087 vw		2092 m		
~2155	2116 s	2116 s	2117 s P	2120 s	$\nu_3(a_1)$ fund	
	2140 w, sh	2133 m	2136 w, sh§	2136 m	$\nu_2 - \nu_{14} = 2144$	E
				2180 w, sh	$\nu_4 + \nu_6 = 2183$	A_1
		2201 vw		2201 m	$\nu_3 + \nu_{14} = 2206$	E
	2227 m, sh				hot band or ^{13}C	
~2240	2234 vs	2235 vs	2233 vs P	2233 vs	$\nu_2(a_1)$ fund	
		2256 vw		2261 w, sh		
				2305 w, sh		
	2315 vw				$\nu_2 + \nu_{14} = 2324$	E
	2331 vw				$\nu_3 + \nu_{13} = 2330$	E
	2378 vw, sh			2374 w	$\nu_4 + \nu_{10} = 2395$	E
	2395 m	2396 m	2396 m P	2396 s	$2\nu_5 = 2396$	A_1
				2428 m	$\nu_3 + \nu_7 = 2426$	A_1
	2446 vw	2443 w		2452 vw	$\nu_2 + \nu_{13} = 2448$	E
			2535 vw	2542 w	$\nu_2 + \nu_7 = 2544$	A_1

Table 3. (*continued*)

Gas	Infrared Solution (CCl_4)	Solid	Raman Solution†	Solid	Interpretation*	
	2571 w	2566 w		2566 vw	$\left\{\begin{array}{l}\nu_2 + \nu_{12} = 2567\\ \nu_4 + \nu_5 = 2572\end{array}\right.$	E A_1
			2671 vw		$\nu_2 + \nu_{11} = 2699$	E
				2704 vw, sh		
	2731 w			2729 w	$2\nu_4 = 2748$	A_1
~2865	2841 s		2841 w	2832 m	$2\nu_9 = 2864$	$A_1 + E$
$\left.\begin{array}{l}\sim 2930\\ \sim 2935\end{array}\right\}\parallel$	2915 vs	2908 m	2913 s P	2908 s	$\nu_1(a_1)$ fund	
~2975 ⊥ ∥	2960 m	2956 m		2957 s	$\nu_8(e)$ fund	
	2996 vw	2995 w		2995 w	$\nu_1 + \nu_{14} = 3005$	E
	3025 w	3026 w			$\nu_2 + \nu_6 = 3043$	A_1
	3152 vw					
		3249 vw				
	3312 w	3315 w				
	3410 vw	3413 vw				

Footnotes: see Table 1.

Table 4. Observed fundamental vibrations for $CH_3—C\equiv C—C\equiv C—X$ (X=H, Cl, Br, I)*

Species		H	Species		Cl	Br	I†	Approx. motion
a_1	ν_1	3333						$\equiv$C—H stretch
	ν_2	2935	a_1	ν_1	2935	2933	2915	CH_3 sym. stretch
	ν_3	2239		ν_2	2257†	2256	2234	C$\equiv$C sym. stretch
	ν_4	2071		ν_3	2175	2158	2116	C$\equiv$C asym. stretch
	ν_5	1385		ν_4	1381	1381	1374	CH_3 sym. def.
	ν_6	1150		ν_5	1228	1210	1198	C—C asym. stretch
	ν_7	696		ν_6	862	815	809	C—C sym. stretch
				ν_7	437†	356†	310	C—X stretch
e	ν_8	2977	e	ν_8	2977	2975	2960	CH_3 asym. stretch
	ν_9	1446		ν_9	1446	1446	1432	CH_3 asym. def.
	ν_{10}	1029		ν_{10}	1029	1029	1021	CH_3 rock
	ν_{11}	614						C$\equiv$C—H bend
	ν_{12}	484		ν_{11}	457	460	465	asym. skeletal bend
	ν_{13}	324†		ν_{12}	339	332	333	sym. skeletal bend
				ν_{13}	241†	223†	212	C$\equiv$C—X bend
	ν_{14}	150†		ν_{14}	101†	92†	90	skeletal bend

* Frequencies from vapour phase unless otherwise indicated.
† Solution frequencies.

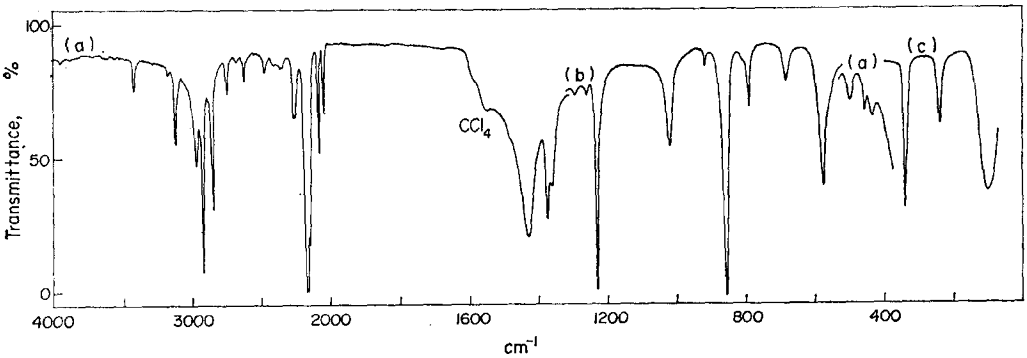

Fig. 1. Infrared spectrum of $CH_3—C\equiv C—C\equiv C—Cl$. (a) CCl_4, (b) CS_2 and (c) pentane solutions.

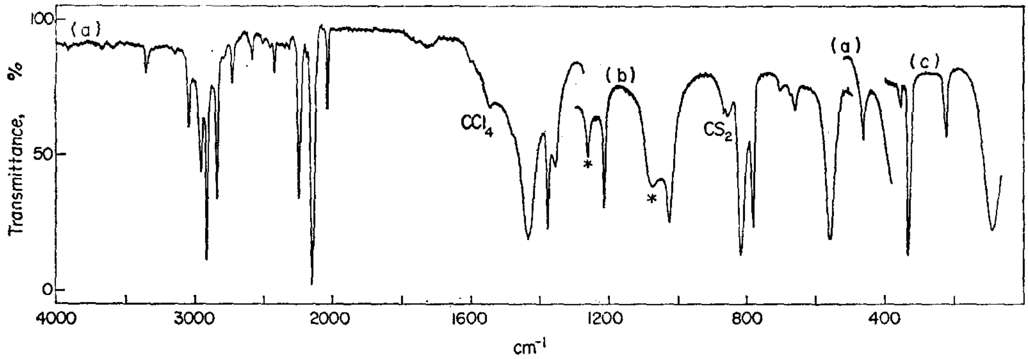

Fig. 2. Infrared spectrum of CH_3—C≡C—C≡C—Br. (a) CCl_4, (b) CS_2 and (c) pentane solutions. Bands marked with * result from impurities.

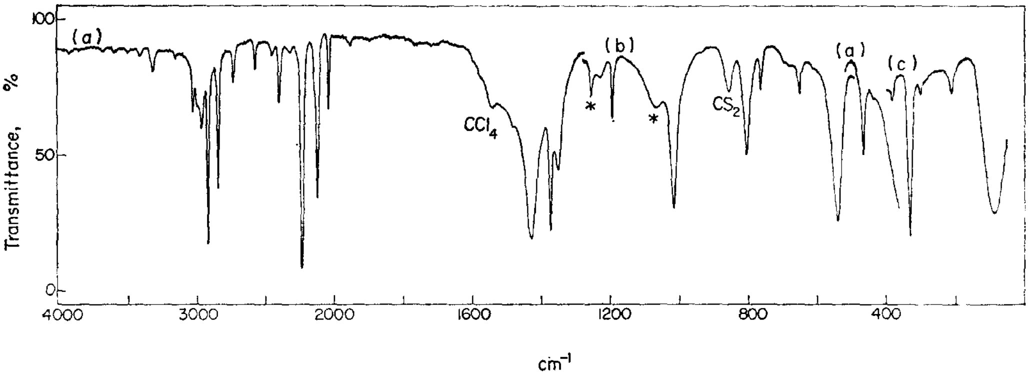

Fig. 3. Infrared spectrum of CH_3—C≡C—C≡C—I. (a) CCl_4, (b) CS_2 and (c) pentane solutions. Bands marked with * result from impurities.

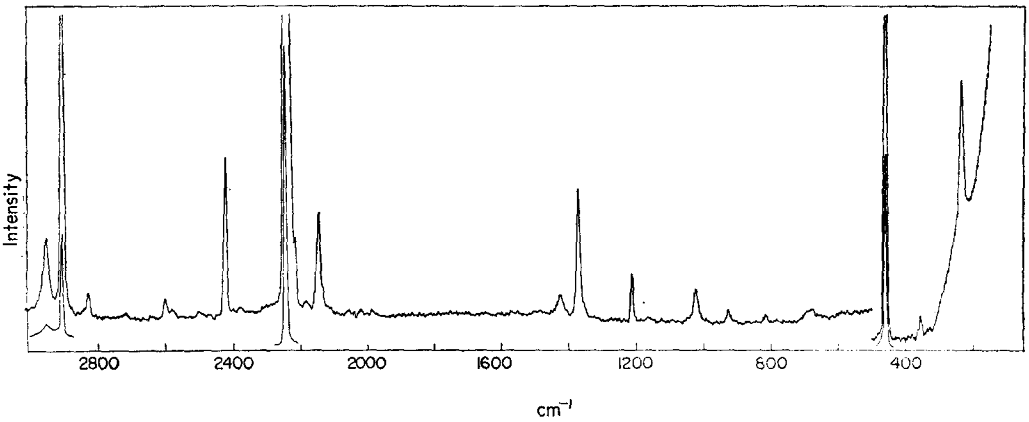

Fig. 4. Raman spectrum of CH_3—C≡C—C≡C—Br. CCl_4 solution: 4000–1000 cm^{-1}, C_6H_6 solution: 1000–50 cm^{-1}.

700–1500 cm^{-1}

The two C—C stretching vibrations, the CH_3 rocking mode and the two CH_3 deformations were expected in this region. Of these fundamentals the two former occurred as medium or strong i.r. bands in the regions 800–860 and 1200–1240 cm^{-1}. Since both vibrations belong to the same species further assignment of the two bands to the symmetric and antisymmetric mode, respectively, was based on the normal coordinates. These were calculated using a published computer program [26] in a modified form [27]. A constant position for the CH_3 rocking motion in all the three molecules was indicated by the force constant calculations. Identification of this mode near 1030 cm^{-1} was aided by the resolved fine structure observed for (H) and (Cl).

1900–2300 cm^{-1}

The two C≡C stretches gave rise to a very strong Raman band (2230–2260 cm^{-1}) and a weaker band (2110–2180 cm^{-1}), suggesting the former frequency as the symmetric mode. In (Cl) and (Br) the lower frequency was associated with the stronger i.r. band, as expected for the antisymmetric mode, whereas the intensities were reversed in (I). The assignment indicated by the Raman intensities was supported by the calculated normal coordinates. Also the linear halodiacetylenes

$$\mathrm{H{-}C{\equiv}C{-}C{\equiv}C{-}}X$$

(X = Cl, Br and I) have been found to have the symmetric mode at the higher frequency [6].

2300–3000 cm^{-1}

Three medium or strong i.r. bands occurred near 2860, 2930 and 2970 cm^{-1} in the vapour. The latter showed resolved rotational structure indicative of the degenerate CH_3 stretching mode, whereas the former was ascribed to an overtone $2\nu_9$ in weak Fermi resonance with the symmetric mode at 2930 cm^{-1} [28].

ROTATIONAL STRUCTURE OF PERPENDICULAR BANDS

The resolved rotational structure of the e-type CH_3 stretching and bending vibrations, ν_8 and ν_9, were examined in (H), (Cl), (Br) and (I). The weaker bands associated with ν_{10}, the CH_3 rocking motion, could not be studied in the less volatile compounds (Br) and (I) at the maximum path length of 1 m. The Q branches of the sub-bands that arise from the $\Delta K = \pm 1$, $\Delta J = 0$ transitions are given by the expression [25]:

$$\begin{aligned}\nu_0^{\mathrm{sub}} &= \nu_0 + [A'(1-\zeta_i)^2 - B'] \\ &\quad \pm 2[A'(1-\zeta_i) - B']K \\ &\quad + [(A'-A'') - (B'-B'')]K^2\end{aligned}$$

To determine ζ_i and ν_0 from this equation we used the A'' and B'' values mentioned in a previous section. With the usual assumption that $B' = B''$ it follows that $(A' - A'') - (B' - B'') = A' - A''$. By the method of least squares determination the observed frequencies have been fitted to equations of the type:

$$\nu^Q = a \pm bK + cK^2.$$

Due to the low intensities and inaccurate readings, (I) was omitted in these calculations. The derived values for ν_0, ζ_i and $A' - A''$ are listed in Table 8, which also contains the corresponding data for related molecules. The uncertainty in our reported frequencies is close to ±0·1 cm^{-1} for narrow bands and the resolution was estimated to ~0·8, ~0·6 and ~0·4 cm^{-1} respectively, in the regions near 3000, 1400 and 1000 cm^{-1}.

ν_8 arises from the antisymmetric CH_3 stretching vibration. As shown for (H) in Fig. 5 it is overlaid on the low frequency side by the parallel CH_3 band. The intensity distribution among the sub-bands permits a choice of either ~3010 or ~2980 cm^{-1} for the $K = 0$ transition. That the latter is probably the correct assignment is shown by the position of the solution peak at ~2960 cm^{-1}. The observed Q branches for all the four molecules are listed in Table 5. A least squares fit gave the equations:

$$\text{(H)}: \nu^Q = 2981{\cdot}9 \pm 9{\cdot}56K - 0{\cdot}03K^2$$

(standard error 0·5 cm^{-1})

$$\text{(Cl)}: \nu^Q = 2981{\cdot}2 \pm 9{\cdot}72K - 0{\cdot}02K^2$$

(standard error 0·3 cm^{-1})

$$\text{(Br)}: \nu^Q = 2979{\cdot}6 \pm 9{\cdot}82K - 0{\cdot}00K^2$$

(standard error 0·5 cm^{-1})

ν_9, the antisymmetric CH_3 deformation is shown for (H) in Fig. 6 and the observed Q branches for all four molecules are given in Table 6. Since the solution value occurs at ~1435 cm^{-1}, the line at 1455 cm^{-1} was chosen for $^RQ_0$, although it is slightly weaker than that at ~1414 cm^{-1}. This assignment is consistent with the expected direction of the phase shift.

The position and intensity distribution of the Q branches are far less regular than those in ν_8.

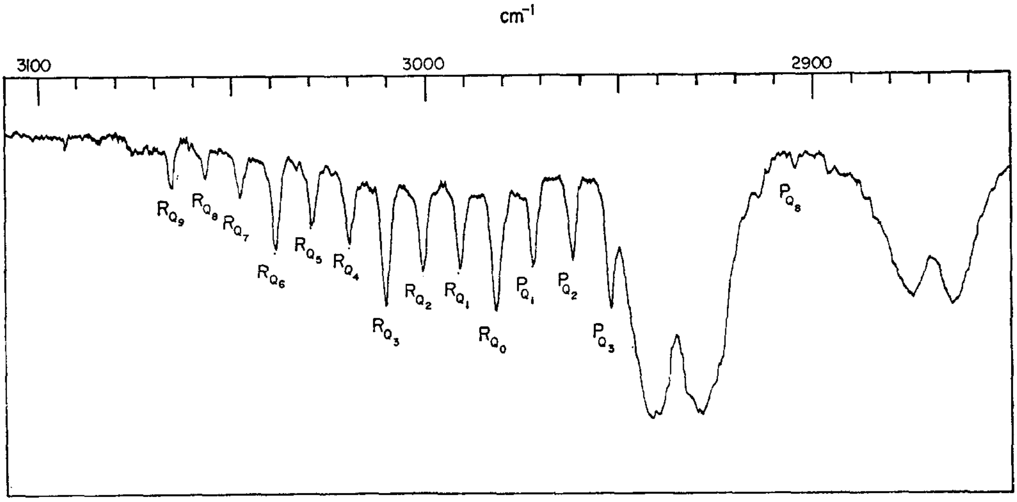

Fig. 5. ν_2 (a_1) and ν_8 (e) bands of $CH_3—C\equiv C—C\equiv C—H$.

Table 5. ν_8 of $CH_3—C\equiv C—C\equiv C—X$ (X = H, Cl, Br, I)

		Band positions in cm^{-1}.						
K-values in		(H)		(Cl)		(Br)		(I)*
^PQ_K	^RQ_K	Obs.	Obs.-calc.	Obs.	Obs.-calc.	Obs.	Obs.-calc.	Obs.
9		∼2895·7†						
8		2904·2	+0·1					
7		∼13·4†						
6						2920·8	+0·1	
5								
4								
3		2952·1	−0·7	2951·5	−0·3	2950·3	+0·1	∼2950·1
2		62·0	−0·5	62·1	+0·4	59·7	−0·3	∼60·3
1		72·1	+0·0	71·6	+0·1	69·4	−0·4	∼71·8
	0	82·2	+0·5	81·2	−0·0	79·4	−0·2	∼78·9
	1	91·2	−0·0	90·8	−0·1	90·1	+0·6	∼89·4
	2	3000·7	−0·0	3000·6	+0·1	99·9	+0·6	∼99·0
	3	10·3	+0·1	9·7	−0·4	3008·5	−0·6	∼3009·0
	4	19·7	+0·1	19·5	−0·2	19·3	+0·4	
	5	29·2	+0·1	29·3	+0·1	28·3	−0·5	
	6	38·7	+0·3	38·8	+0·2	38·7	+0·1	
	7	48·2	+0·4	48·3	+0·3			
	8	57·0	−0·1	57·5	+0·1			
	9	65·0	−0·5	66·4	−0·3			
	10	∼75·0†						
	11	∼84·2†						
	12	∼92·8†						
	13	∼3101·1†						

* No polynomial is fitted to the sub-band frequencies.

† Sub-bands omitted in the calculation.

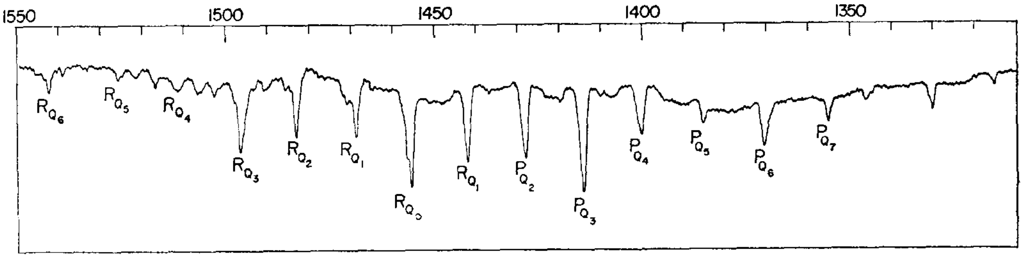

Fig. 6. ν_9 (*e*) band of $CH_3—C{\equiv}C—C{\equiv}C—H$.

As previously shown in $CH_3—C{\equiv}N$ [24] and $CH_3—C{\equiv}C—H$ [25, 29] these anomalies probably arise from the presence of overlapping and perturbing bands. The least perturbed Q branches are fairly well fitted by the expressions:

(H): $\nu^Q = 1455{\cdot}5 \pm 14{\cdot}14K$

(standard error 0·6 cm^{-1})

(Cl): $\nu^Q = 1455{\cdot}3 \pm 14{\cdot}02K$

(standard error 0·2 cm^{-1})

(Br): $\nu^Q = 1455{\cdot}4 \pm 14{\cdot}19K$

(standard error 0·6 cm^{-1})

The square terms in K were omitted because of the large uncertainties.

ν_{10} is associated with the CH_3 rocking motion. The band in (H) is shown in Fig. 7. and Table 7. lists the observed Q branches in (H) and in (Cl). The spacing is rather regular and the assignment of R_{Q_0} to the strongest line is supported by the solution value. An asymmetry or a shoulder appears on the low frequency side of the Q branches, and in (H) the P_{Q_2} and P_{Q_3} bands are resolved into doublets. This sequence of weaker bands may arise from a hot transition as previously observed in $CH_3—C{\equiv}C—H$ [32]. The Q branches of the main series are expressed by the following equations:

(H): $\nu^Q = 1030{\cdot}5 \pm 6{\cdot}30K + 0{\cdot}02K^2$

(standard error 0·3 cm^{-1})

(Cl): $\nu^Q = 1030{\cdot}7 \pm 6{\cdot}19K + 0{\cdot}02K^2$

(standard error 0·3 cm^{-1})

Table 6. ν_9 of $CH_3—C{\equiv}C—C{\equiv}C—X$ (X = H, Cl, Br, I)

K-values in		Band positions in cm^{-1}. (H)*		(Cl)†		(Br)		(I)‡
P_{Q_K}	R_{Q_K}	Obs.	Obs.-calc.	Obs.	Obs.-calc.	Obs.	Obs.-calc.	Obs.
13		~1271·9						
12		~86·2						
11		1301·0						
10		15·5		1315·10				
9		30·43		29·30				
8		46·15		43·94				
7		55·12	−1·82	58·85				
6		70·68	−0·31	75·37				
5		85·25	+0·22	85·30	+0·16			
4		1400·13	+1·05	99·00	−0·17	1398·6	−0·1	~1398·4
3		14·15	+1·02	1413·20	+0·01	1413·1	+0·2	~1412·6
2		28·03	+0·86	27·25	+0·04	27·4	+0·3	~27·0
1		41·85	+0·63	41·00	−0·23	41·0	−0·3	~40·7
	0	55·37	+0·11	55·44	+0·19	54·6	−0·9	~54·4
	1	68·70	−0·61	67·37		70·2	+0·6	~69·8
	2	83·18	−0·18	84·75		84·1	+0·3	~83·7
	3	96·43	−0·97	98·82		97·8	−0·2	
	4	1511·48		1514·02		1512·3	+0·1	
	5	26·00		31·65				
	6	42·43		46·05				

* Sub-bands from R_{Q_3} to P_{Q_7} are used in the calculation.

† Sub-bands from R_{Q_0} to P_{Q_5} are used in the calculation.

‡ No polynomial is fitted to the sub-band frequencies.

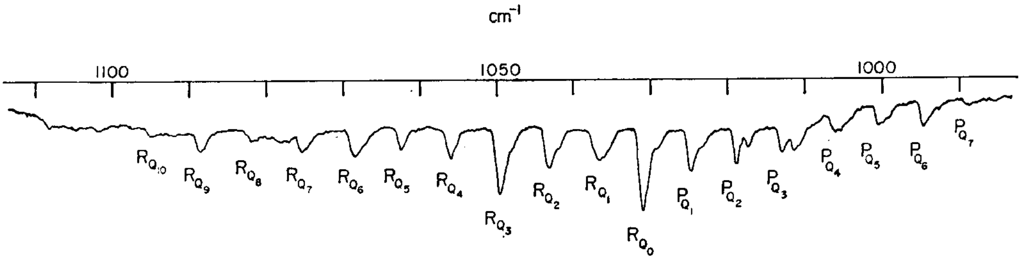

Fig. 7. ν_{10} (*e*) band of $CH_3—C\equiv C—C\equiv C—H$.

Table 7. ν_{10} of $CH_3—C\equiv C—C\equiv C—X$ (X = H, Cl)

K-values in ^PQ_K	^RQ_K	Band positions in cm⁻¹. (H) Obs.	(H) Obs.-calc.	(Cl) Obs.	(Cl) Obs.-calc.
7		988·5	+0·1		
6		94·4	+0·1		
5		1000·2	−0·1		
4		5·8	−0·5	1005·9	+0·2
3		12.7	+0·4	11·3	−0·5
2		18·7	+0·3	18·3	+0·3
1		24·6	+0·1	24·1	−0·1
	0	30·9	+0·2	30·7	+0·2
	1	36·4	−0·5	36·9	+0·1
	2	43·0	−0·2	43·7	+0·5
	3	49·4	−0·1	49·2	−0·5
	4	55·9	+0·1	56·0	−0·1
	5	62·4	+0·2	62·6	−0·1
	6	68·4	−0·2	69·1	−0·1
	7	75·2	+0·1	1076·1	+0·2
	8	81·7	+0·1		
	9	88·5	+0·3		
	10	1094·4	−0·4		

The ζ_i values for the remaining *e*-type bands may be estimated from the sum rule [30]:

$$\sum_i \zeta_i = (\text{No. of axial atoms}) - 2 + \frac{B''}{2A''}$$

Assuming a value of 0·40 for ζ_{10} in (Br) the sum $\zeta_{11} + \zeta_{12} + \zeta_{13} + \zeta_{14} = 3{\cdot}86$ in (H), (Cl) and (Br), which places each of the individual ζ_i values between 0·86 and 1. These high values imply a small spacing between the *Q* branches, in accordance with our observations of broad absorption bands with no fine structure for these fundamentals. Fairly good agreement is found for the ζ_i values obtained in the present study and those derived from the force field [2].

Table 8 shows the great similarity in the ν_0 and ζ_i values for the respective CH_3 vibrations in the series (H), (Cl), (Br) and (I). The data indicate that the small variations which have been observed in the $CH_3—C\equiv C—X$ series have vanished in the 1,3–pentadiynes due to the larger separation of the *X* substituent from the CH_3 group.

THERMODYNAMIC FUNCTIONS

The thermodynamic functions were calculated from vapour phase data and from rotational constants given in the previous section. These calculations which include 1,3-pentadiyne, were made for atmospheric pressure in the rigid rotor, harmonic oscillator approximation [31]. Gas values for ν_{14}, the lowest bending mode were obtained from difference bands. Gas frequencies which escaped observation, mainly in (I), were estimated from the corresponding phase shifts in the more volatile members of the series. The results are listed in Table 9.

Table 8. ν_0, ζ_i and ($A'—A''$) values for $CH_3—C\equiv C—C\equiv C—X$ (X = H, Cl, Br, I) and related molecules*

Sample	Asym. methyl stretch ν_0	ζ_i	($A'—A''$)	Asym. methyl bend ν_0	ζ_i	($A'—A''$)	Methyl rock ν_0	ζ_i	($A'—A''$)
CH_3·CCCC·H	2977·2	0·08	−0·02	1445·8	−0·34	—	1028·9	0·40	+0·02
CH_3·CCCC·Cl	2976·7	0·08	−0·02	1445·8	−0·34	—	1028·7	0·40	+0·02
CH_3·CCCC·Br	2975·1	0·07	0·00	1445·9	−0·35	—	—	—	—
CH_3·CCCC·I	~2975	—	—	~1445	—	—	—	—	—
CH_3·CC·H [25, 29]	2980·8	0·06	−0·021	1450·88	−0·311	−0·053	1036·03	0·403	+0·023
CH_3·CC·D [32]	2980·1	0·075	−0·028	1451·8	−0·32	−0·023	1051·73	0·40	+0·021
CH_3·CC·Cl [3]	2979·9	0·042	−0·046	1453·78	−0·357	−0·028	1034·5	0·40	+0·005
CH_3·CC·Br [4]	2978·8	0·051	−0·044	1451·6	−0·35	−0·014	1034·0	0·393	−0·022
CH_3·CC·I [4]	2977·5	0·072	−0·020	1450·4	−0·336	−0·024	1032·7	0·383	—
CH_3·CC·CN [33]	2986·5	0·047	−0·035	1445·33	−0·370	−0·008	1029·76	0·408	+0·026

* The approximation $B' = B''$ is assumed.

Table 9. Thermodynamic functions for $CH_3-C\equiv C-C\equiv C-X$ (X = H, Cl, Br and I). Heat content H°, free energy G°, entropy S° and heat capacity C_p°. The units are cal deg^{-1} mole^{-1}*

	$CH_3-C\equiv C-C\equiv C-H$					$CH_3-C\equiv C-C\equiv C-Cl$			
T(°K)	$-(G^\circ - H^\circ)/T$	S°	$(H^\circ - H_0^\circ)/T$	C_p°	T(°K)	$-(G^\circ - H^\circ)/T$	S°	$(H^\circ - H_0^\circ)/T$	C_p°
100	43·28	52·69	9·40	11·90	100	47·73	58·41	10·68	14·22
200	50·59	62·60	12·01	17·26	200	56·21	70·33	14·11	20·39
273·16	54·62	68·50	13·88	20·66	273·16	60·94	77·16	16·23	23·51
298·16	55·86	70·36	14·50	21·70	298·16	62·38	79·26	16·88	24·44
300	55·95	70·49	14·54	21·78	300	62·49	79·41	16·92	24·51
400	60·45	77·27	16·82	25·45	400	67·69	86·93	19·25	27·85
500	64·43	83·29	18·86	28·49	500	72·20	93·46	21·26	30·67
600	68·03	88·72	20·69	31·04	600	76·24	99·27	23·03	33·08
	$CH_3-C\equiv C-C\equiv C-Br$					$CH_3-C\equiv C-C\equiv C-I$			
T(°K)	$-(G^\circ - H^\circ)/T$	S°	$(H^\circ - H_0^\circ)/T$	C_p°	T(°K)	$-(G^\circ - H^\circ)/T$	S°	$(H^\circ - H_0^\circ)/T$	C_p°
100	49·59	60·47	10·88	14·64	100	50·56	61·60	11·04	14·94
200	58·26	72·69	14·43	20·80	200	59·36	74·01	14·65	21·01
273·16	63.08	79·64	16·56	23·84	273·16	64·25	81·02	16·76	23·98
298·16	64·56	81·77	17·21	24·75	298·16	65·75	83·16	17·41	24·88
300	64·67	81·92	17·26	24·82	300	65·86	83·31	17·45	24·94
400	69·96	89·52	19·57	28·08	400	71·20	90·94	19·74	28·17
500	74·54	96·09	21·55	30·86	500	75·82	97·53	21·71	30·93
600	78·63	101·94	23·31	33·23	600	79·94	103·38	23·45	33·29

* Values employed for ν_{14}: (H) 139, (Cl) 83, (Br) 79 and (I) 76 cm^{-1}.

Acknowledgement—We are indebted to F. M. Nicolaisen, Chemical Laboratory V, H. C. Ørsted Institute, Copenhagen for his help in recording the far i.r. spectra. The skilful technical assistance of E. R. Iversen and the financial support from Nansenfondet (E. K. -J) are gratefully acknowledged.

REFERENCES

[1] J. Lamotte, J. C. Lavalley and R. Romanet, *J. Chim. Phys.* **70,** 1077 (1973).
[2] A. Rogstad, L. Benestad and S. J. Cyvin, *J. Mol. Structure* In press.
[3] D. W. Davidson and H. J. Bernstein, *Can. J. Chem.* **33,** 1226 (1955) and references cited.
[4] R. A. Nyquist, *Spectrochim. Acta.* **21,** 1245 (1965).
[5] P. Klaboe, E. Kloster-Jensen and S. J. Cyvin, *Spectrochim Acta* **23A,** 2733 (1967).
[6] B. Minasso and G. Zerbi, *J. Mol. Structure* **7,** 59 (1971).
[7] E. Kloster-Jensen, *Tetrahedron* **27,** 33 (1971).
[8] E. Heilbronner, V. Hornung, J. P. Maier and E. Kloster-Jensen, *J. Amer. Chem. Soc.* **96,** 4252 (1974).
[9] J. B. Armitage, E. R. H. Jones and M. C. Whiting, *J. Chem. Soc.* 1993 (1952).
[10] J. B. Armitage, E. R. H. Jones and M. C. Whiting, *J. Chem. Soc.* 44 (1951).
[11] H. H. Schlubach and V. Wolf, *Ann.* **568,** 141 (1950).
[12] C. H. Prévost, *Compt. rend.* **182,** 854 (1926).
[13] W. Chodkiewicz, *Ann. Chim.* (*Paris*), **2,** 819 (1957).
[14] F. Bohlmann and P. Herbst, *Chem. Ber.* **91,** 1631 (1958).
[15] E. R. H. Jones, G. Lowe and P. V. R. Shannon *J. Chem. Soc. C* 139 (1966).
[16] E. K. Plyler, A. Danti, L. R. Blaine and E. D. Tidwell, *J. Res. Natl. Bur. Stand.* **64,** no. 1 (1960).
[17] *Tables of Wavenumbers for the Calibration of Infrared Spectrometers, I.U.P.A.C. Report,* Butterworth (1961).
[18] J. W. Levin, *Spectrochim. Acta,* **25A,** 1157 (1969).
[19] G. A. Heath, L. F. Thomas, E. J. Sherrard and J. Sheridan, *Disc. Faraday Soc.* **19,** 38 (1955).
[20] R. Trambarulo and W. Gordy, *J. Chem. Phys.* **18,** 1613 (1950).
[21] L. F. Thomas, E. I. Sherrard and J. Sheridan, *Trans. Faraday Soc.* **51,** 619 (1955).
[22] S. L. Gerhard and D. M. Dennison, *Phys. Rev.* **43,** 197 (1933).
[23] W. A. Seth-Paul and G. Djikstra, *Spectrochim. Acta* **23A,** 2861 (1967).
[24] I. Nakagava and T. Shimanouchi, *Spectrochim. Acta* **18,** 513 (1962).
[25] R. K. Thomas and H. W. Thompson, *Spectrochim. Acta* **24A,** 1337 (1968).
[26] W. D. Gwinn, *J. Chem. Phys.* **55,** 477 (1971).
[27] A. Bjørseth and R. Stølevik, unpublished work.
[28] J. C. Lavalley and N. Sheppard, *Spectrochim. Acta* **28A,** 2091 (1972).
[29] J. L. Duncan, I. J. Wright and D. Ellis, *J. Mol. Spectry.* **37,** 394 (1971).
[30] D. R. J. Boyd and H. C. Longuet-Higgins, *Proc. Roy. Soc.* (*London*), **A213,** 55 (1952).
[31] G. Herzberg, *Infrared and Raman Spectra of Polyatomic Molecules,* Van Nostrand, Princeton, (1945).
[32] R. K. Thomas and H. W. Thompson, *Spectrochim. Acta* **24,** 1353 (1967).
[33] R. Tubino, G. Dellepiane and G. Zerbi, *J. Chem. Phys.* **50,** 621 (1969).